

Orbital effect of an in-plane magnetic field on quantum transport in chaotic lateral dots

Vladimir I. Fal'ko¹ and Tomas Jungwirth^{2,3}

¹*Physics Department, Lancaster University, LA1 4YB Lancaster, United Kingdom*

²*Institute of Physics, Czech Academy of Sciences, Prague, Czech Republik*

³*Physics Department, University of Texas, Austin, Texas*

(Received 15 November 2001; published 7 February 2002)

We show that an in-plane magnetic field is able to break time-reversal symmetry of the orbital motion of electrons in two-dimensional semiconductor structures, due to the momentum-dependent inter-subband mixing, which results in suppression of weak localization effect. Then, we analyze the influence of the in-plane field on weak localization correction and universal fluctuations of conductance in large-area chaotic semiconductor quantum dots.

DOI: 10.1103/PhysRevB.65.081306

PACS number(s): 73.23.-b, 72.15.Rn, 73.20.Fz, 73.50.-h

A high sensitivity of phase-coherent transport through quantum dots to external perturbations has recently enabled one to transform studies of mesoscopic effects¹⁻⁴ into a spectroscopic tool for detecting tiny energetic changes in the electron gas⁵ and for studying electron dephasing and inelastic relaxation rates.^{6,7} A convenient object,⁸ once used as a mesoscopic thermometer,⁹ consists of a lateral semiconductor dot weakly coupled to the reservoirs via two leads, l and r , each with $N_{l,r} \geq 1$ open conducting channels, and, therefore, quantum conductances $g_{l,r} = (2e^2/h)N_{l,r}$. Information concerning fine energetic characteristics of single-particle electron states in a dot can be extracted from the variance and parametric correlations of universal conductance fluctuations (UCF), $\delta g = g - \langle\langle g \rangle\rangle$, measured as random oscillations of the dot conductance, g around the mean value, $\langle\langle g \rangle\rangle = g_l g_r / (g_l + g_r) + g_{\text{WL}}$, upon variation of a perpendicular magnetic field,^{1,3} the Fermi energy,^{2,3} or the dot shape⁸ and combined with the analysis of parametric dependences of the weak localization part in the average dot conductance, g_{WL} .

Energetic resolution of such a spectroscopy is set by the level broadening of single-particle states in a particular device, which is limited by the carrier escape into the leads,

$$\tau_{\text{esc}}^{-1} = (N_l + N_r)\Delta/h,$$

where $\Delta = 2\pi\hbar^2/mS$ is the mean level spacing of single-particle states of spin-polarized electrons with mass m in a dot with area S . The use of larger dots with weaker coupling to the leads increases the sensitivity of the dot conductance to the variation of external parameters. The use of larger dots also enables one to assess directly the low excitation energy characteristics of the two-dimensional (2D) electron gas, since the electron properties in $1 \div 10 \mu\text{m}^2$ -area dots containing $10^3 - 10^4$ particles are less affected by the confinement effects. Recently, large area dots were used for studying spin polarization of a 2D electron gas.⁵ In order to enhance coupling between a magnetic field and electron spin, J. Folk *et al.*⁵ used a magnetic field finely tuned to lay exactly parallel to the plane of 2D electrons and observed a suppression of the variance $\langle\langle \delta g^2(B_{\parallel}) \rangle\rangle$ by an in-plane field B_{\parallel} much stronger than that associated with a mere spin splitting, which can be understood in terms of spin-orbit coupling in

the 2D gas.^{10,11} It has been observed in further studies¹² that an application of an in-plane magnetic field also results in a complete suppression of a weak localization part of the conductance, which cannot be attributed solely to the interplay between spin-orbit coupling and Zeeman splitting,¹¹ but requires lifting the time-reversal symmetry of the orbital motion by the in-plane field. In the present publication, we show that, due to a finite extent λ_z of the electron wave function across the heterostructure, even a perfectly tuned in-plane magnetic field may break time-reversal symmetry of the orbital motion of effectively 2D electrons. We compute the rate of such time-reversal symmetry breaking in 2D semiconductor structures and, then, determine the range of fields B_{\parallel} that would affect WL and UCF's in experimentally studied quantum dot devices,⁵ in addition to spin-related phenomena.

The Lorentz force generated by a planar field on electrons moving across \mathbf{B}_{\parallel} within the 2D plane mixes up the electron motion along and across the confinement direction, thus resulting in the electron momentum, \mathbf{p} dependent subband mixing and, therefore, in a modification of the 2D dispersion,^{13,14} $E(p) \rightarrow E(\mathbf{B}_{\parallel}, \mathbf{p})$. In particular, (a) the 2D electron mass increases in the direction perpendicular to \mathbf{B}_{\parallel} , whereas (b) in heterostructures which have no inversion symmetry in the form of confining potential, \mathbf{B}_{\parallel} also lifts the $\mathbf{p} \rightarrow -\mathbf{p}$ symmetry in the dispersion law:¹³ $E(\mathbf{B}_{\parallel}, \mathbf{p}) - E(\mathbf{B}_{\parallel}, -\mathbf{p}) \propto (\mathbf{p} \cdot [\mathbf{B}_{\parallel} \times \mathbf{l}_z])^3 \neq 0$. The change in dispersion (b) has potential to reduce the fundamental symmetry of chaotic dot from orthogonal (o) to unitary (u), as a perpendicular magnetic field would do. The efficiency of time-reversal symmetry breaking by an in-plane magnetic field can be characterized using the rate $\tau_{B_{\parallel}}^{-1} \sim bB_{\parallel}^6 + aB_{\parallel}^2$ specified in Eq. (8). A similar conclusion has recently been made in Ref. 15. Without spin-related effects, this parameter would determine the value of the WL correction, $g_{\text{WL}}(B_{\parallel}) \equiv \langle\langle g(B_{\parallel}) \rangle\rangle - \langle\langle g \rangle\rangle_u$ and of the variance of UCF, $\langle\langle \delta g^2(B_{\parallel}) \rangle\rangle$, as compared to their nominal values, $g_{\text{WL}}(0) \equiv \langle\langle g \rangle\rangle_o - \langle\langle g \rangle\rangle_u$ and $\langle\langle \delta g^2 \rangle\rangle_u$.^{16,17}

$$g_{\text{WL}}(B_{\parallel}) = g_{\text{WL}}(0) [1 + \tau_{B_{\parallel}}^{-1} / \tau_{\text{esc}}^{-1}]^{-1}; \quad (1)$$

$$\langle\langle \delta g^2(B_{\parallel}) \rangle\rangle = \langle\langle \delta g^2 \rangle\rangle_u \{1 + [1 + \tau_{B_{\parallel}}^{-1} / \tau_{\text{esc}}^{-1}]^{-2}\}.$$

The latter parameters can be measured as the UCF's fingerprints in the "shape of a dot" space in multigate devices,⁸ or by varying the Fermi energy in backgated dots. The rise in the mass anisotropy upon the increase of B_{\parallel} would also manifest itself: as a change in a UCF pattern scanned as a function of a perpendicular magnetic field. A varying dispersion relation for electrons studied at different fields, $B_{\parallel 1}$ and $B_{\parallel 2}$, can be characterized using the rate $\tau_d^{-1}(B_{\parallel 1}, B_{\parallel 2}) \propto (B_{\parallel 1}^2 - B_{\parallel 2}^2)^2$ in Eq. (6), which can be used to describe auto-correlation properties of a full B_{\perp} -dependent UCF pattern,

$$\frac{\langle\langle \delta g(B_{\parallel 1}) \delta g(B_{\parallel 2}) \rangle\rangle_u}{\langle\langle \delta g^2 \rangle\rangle_u} = \left[1 + \frac{\tau_d^{-1}(B_{\parallel 1}, B_{\parallel 2})}{\tau_{\text{esc}}^{-1}} \right]^{-2}. \quad (2)$$

The effective 2D Hamiltonian for electrons in a heterostructure with a potential profile $V(z)$ and in the presence of an in-plane magnetic field can be obtained from the 3D Hamiltonian,

$$\hat{H}_{3D} = -\frac{\hbar^2 \partial_z^2}{2m} + V(z) + \frac{\left(-i\hbar \nabla - \frac{e}{c} \mathbf{A} \right)^2}{2m} + u(\mathbf{r}, z), \quad (3)$$

using the plane wave representation, $\Psi_{\mathbf{p}} = e^{i\mathbf{p} \cdot \mathbf{r}/\hbar} \varphi_{0\mathbf{p}}(z)$ for the lowest subband electrons. Here, $\mathbf{A} = (z - z_0) \mathbf{B}_{\parallel} \times \mathbf{I}_z$ is the vector potential, $z_0 = \langle 0 | z | 0 \rangle$ is the center of mass position of the electron wave function $|0\rangle \equiv \varphi_0^{(0)}(z)$ in the lowest subband for $B_{\parallel} = 0$, and $u(\mathbf{r}, z)$ is a combination of Coulomb potential of impurities and lateral potential forming the quantum dot. Due to mixing between subbands $|0\rangle$ and $|n\rangle > 0$ by an in-plane magnetic field, z -dependent components $\varphi_{0\mathbf{p}}(z)$ are different for different in-plane momenta, \mathbf{p} , and we use both the perturbation theory analysis¹⁸ and a numerical self-consistent-field technique to find $\varphi_{0\mathbf{p}}(z)$ and the energy $E(\mathbf{B}_{\parallel}, \mathbf{p})$ for each plane wave state.

For a weak or intermediate-strength magnetic field \mathbf{B}_{\parallel} , the effective 2D Hamiltonian takes the form

$$\hat{H}_{2D} = \frac{\mathbf{p}^2}{2m} - p_{\perp}^2 \gamma(B_{\parallel}) + p_{\perp}^3 \beta(B_{\parallel}) + u(\mathbf{r}). \quad (4)$$

In Eq. (4), $\mathbf{p} = -i\hbar \nabla - (e/c) \mathbf{a}(\mathbf{r})$ is a purely 2D momentum operator, and $p_{\perp} = \mathbf{p} \cdot [\mathbf{B}_{\parallel} \times \mathbf{I}_z] / B_{\parallel}$ is its component perpendicular to \mathbf{B}_{\parallel} . Two additional terms in the free-electron dispersion part of \hat{H}_{2D} are the result of the p_{\perp} -dependent inter-subband mixing. The first of them lifts rotational symmetry by causing an anisotropic mass enhancement.¹³ It increases the 2D density of states and, for a 2D gas with a fixed sheet density, it reduces the Fermi energy calculated from the bottom of the 2D conduction band, $E_F(B_{\parallel}) = E_F^0 - [\gamma(B_{\parallel})/2] p_F^2$. A cubic term in \hat{H}_{2D} is related to the time-reversal symmetry breaking by B_{\parallel} . Note that, depending on the choice of a gauge, one may also generate a linear p_{\perp} term, but this one can be eliminated by a trivial gauge transformation. A perturbation theory analysis of this problem is discussed in Ref. 18, and for a moderate field it results in the parametric dependences $\gamma \sim m^{-1} (\lambda_z / \lambda_B)^4$ and $\beta \sim (\lambda_z / m\hbar) (\lambda_z / \lambda_B)^6$.

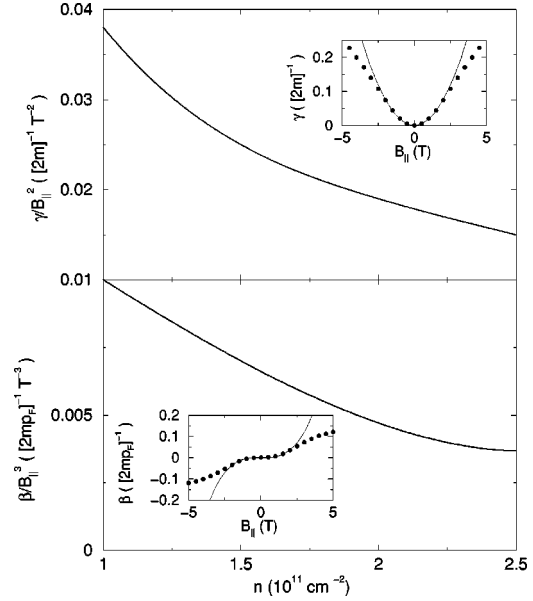


FIG. 1. Calculated dependence of parameters γ and β on the sheet density of 2D electrons. Insets show the effect of B_{\parallel} on symmetric, $[E(p_{\perp}) + E(-p_{\perp})]/2$ and antisymmetric, $[E(p_{\perp}) - E(-p_{\perp})]/2$ parts of the 2D electron dispersion in a broader range of B_{\parallel} , where a perturbative expansion is not applicable.

To obtain quantitative estimates for parameters γ and β , we evaluated the electron dispersion at in-plane magnetic fields using a full self-consistent numerical method. The quantum-well confining potential $V(z)$ was constructed using the nominal growth parameters of the sample studied in Ref. 5 which was an $\text{Al}_{0.34}\text{Ga}_{0.66}\text{As}/\text{GaAs}$ heterojunction. $V(z)$ also included Hartree and exchange-correlation potentials generated by the free carriers in the quantum well. The Hartree potential was derived from the z -dependent 3D density of electrons by numerical solution of the Poisson equation. The exchange-correlation term was calculated within the local-density approximation.¹⁹ A flat-band boundary condition was used, i.e., we assumed that the electric field produced by donors in the $(\text{Al}, \text{Ga})\text{As}$ barrier is screened out in the GaAs buffer layer by the 2D electron gas. In each loop of the self-consistent procedure we solved numerically the Schrödinger equation with the Hamiltonian in Eq. (3) to get the 3D electron density, neglecting $u(\mathbf{r}, z)$. Then, a new $V(z)$ was constructed, which entered the next loop of the procedure until the self-consistency condition was achieved. The numerically obtained dependences of γ and β on the in-plane magnetic field for an electron sheet density of $2 \times 10^{11} \text{ cm}^{-2}$ are shown in insets of Fig. 1. At low fields, $\gamma \sim B_{\parallel}^2$ and $\beta \sim B_{\parallel}^3$, as anticipated in the perturbation theory treatment. The proportionality coefficients are plotted in Fig. 1 versus the electron sheet density. Both the effective-mass renormalization in the quadratic term of energy dispersions and the time-reversal symmetry breaking cubic term are larger at lower 2D electron gas densities, due to a weaker confining electric field (i.e., longer λ_z).

In \hat{H}_{2D} in Eq. (4), disorder is incorporated in the form of a scattering potential $u(\mathbf{r}) \approx \langle 0 | u(\mathbf{r}, z) | 0 \rangle$. This can be characterized by the value of the mean free path, $l \gg \hbar / p_F$, or a

momentum relaxation time τ related to the diffusion coefficient $D = v_F^2 \tau / 2$. The modification of the electron density of states by B_{\parallel} only slightly affects the value of the electron mean free path. The presence of a parallel field also changes the symmetry of Born amplitudes of scattering between plane waves $\Psi_{\mathbf{p}} = e^{i\mathbf{p} \cdot \mathbf{r} / \hbar} \varphi_{0\mathbf{p}}(z)$, $f_{\mathbf{p}\mathbf{p}'} = \langle \Psi_{\mathbf{p}} | u(\mathbf{r}, z) | \Psi_{\mathbf{p}'} \rangle$. Due to the momentum-dependent subband mixing, $f_{\mathbf{p}\mathbf{p}'}$ acquires an addition, $f_{\mathbf{p}\mathbf{p}'} = f_{\mathbf{p}\mathbf{p}'}^{(0)} \{1 + (p_{\perp} + p'_{\perp}) B_{\parallel} \zeta\}$, where

$$\zeta = \frac{e}{mc} \sum_{n \geq 1} \frac{\langle 0 | u(\mathbf{p} - \mathbf{p}', z) | n \rangle \langle n | z | 0 \rangle}{\langle 0 | u(\mathbf{p} - \mathbf{p}', z) | 0 \rangle \varepsilon_n - \varepsilon_0},$$

which is equivalent to the presence of a random gauge field in the effective 2D Hamiltonian,^{20,21}

$$\mathbf{a} = 2[\mathbf{B}_{\parallel} \times \mathbf{1}_z] \sum_{n \geq 1} \frac{\langle 0 | u(\mathbf{r}, z) | n \rangle \langle n | z | 0 \rangle}{\varepsilon_n - \varepsilon_0}.$$

The latter can be interpreted as a result of an effective ‘‘curving’’ of a 2D plane by impurities in systems with z -dependent scattering potential, which in the presence of an in-plane magnetic field generates a random effective perpendicular field component, $b_{\perp} = [\text{rota}]_z$. In systems, where scattering is dominated by Coulomb centers behind a spacer and is almost independent of z , a smaller effect may be taken into account, $\delta \mathbf{a} = \eta[\mathbf{B}_{\parallel} \times \mathbf{1}_z][(\mathbf{B}_{\parallel} \times \mathbf{1}_z) \cdot \nabla]^2 u(\mathbf{r})$. However, $\delta \mathbf{a}$ has a negligible influence on the quantum transport characteristics of 2D electrons, as compared to the effect of dispersion.

Quantum transport characteristics of chaotic dots (WL and UCF's) are studied in this paper by modeling dots as 2D billiards filled with a short-range disorder. It has been shown before that the results obtained for a zero-dimensional limit of diffusive systems, $\tau_{\text{esc}} \gg L^2/D$ and $L > l$, are universally applicable to the description of WL and UCF's in a broad variety of quantum chaotic billiards,^{4,22} even in ballistic ones.^{23,4} We also used a semiclassical diagrammatic language to calculate two-particle correlation functions, Cooperons $P_C(\omega; \mathbf{R}, \mathbf{R}')$ and diffusons $P_d(\omega; \mathbf{R}, \mathbf{R}')$.³ These correlation functions emerge in the form of ladder diagrams from the perturbation theory analysis upon averaging over disorder the Kubo-formula conductance. Schematically, the form of a weak localization correction and of the variance and correlation function of UCF can be represented as

$$g_{\text{WL}}(B_{\parallel}) \propto \int d\mathbf{R} W(\mathbf{R}) P_C(0; \mathbf{R}, \mathbf{R})$$

and

$$\begin{aligned} & \langle \langle \delta g(B_{\parallel 1}) \delta g(B_{\parallel 2}) \rangle \rangle \\ & \propto \int d\mathbf{R} d\mathbf{R}' W(\mathbf{R}) W(\mathbf{R}') \sum_{d,c} |P_{d,c}(\omega; \mathbf{R}, \mathbf{R}')|^2, \end{aligned}$$

where $\omega = E_F(B_{\parallel 1}) - E_F(B_{\parallel 2})$, and $E_F(B_{\parallel})$ is the Fermi energy of the 2D gas calculated from the bottom of the 2D conduction band determined in Eq. (4). Dispersionless weight factors $W(\mathbf{R})$ both take care of the particle number conservation upon diffusion inside a dot²⁴ and incorporate coupling parameters to the leads. In the zero-dimensional limit, both g_{WL} and $\langle \langle \delta g(B_{\parallel 1}) \delta g(B_{\parallel 2}) \rangle \rangle$ are dominated by the lowest Cooperon (diffuson) relaxation mode $\tau_{\text{esc}}^{-1} + \tau_{\text{C(d)}}^{-1}$ determined by the interplay of the escape to the reservoirs

and the Cooperon (diffuson) suppression by time-reversal symmetry breaking (the difference in condition of quantum diffusion). The latter effect can be analyzed for an infinite system, where the derivation is simplified by the use of Fourier representation for Cooperons (diffusons).

Using the Fourier form, the equation for the diffuson (Cooperon) correlation function, $\Pi \cdot P_{\text{d(C)}}(\omega, \mathbf{q}) = \tau^{-1}$, can be obtained from the analysis of a kernel ($\hbar = 1$),

$$\Pi(\omega, \mathbf{q}) = 1 - \int \frac{d\mathbf{p}}{2\pi\nu\tau} G_{B_{\parallel 1}}^R(\varepsilon, \mathbf{p}) G_{B_{\parallel 2}}^A(\varepsilon - \omega, \pm[\mathbf{p} - \mathbf{q}]),$$

where sign $+/-$ is related to diffuson (Cooperon), respectively. Disorder-averaged retarded and advanced single-particle Green functions, $G^{R,A}$ correspond to different values of B_{\parallel} . $G^{R,A}$ were calculated perturbatively with respect to all terms containing B_{\parallel} , which relies on the assumption that within the relevant parametric regime the variation of the energy, $\delta E(p_F)$ induced by B_{\parallel} is small in comparison with the scattering rate, $\delta E \ll \hbar/\tau$. The result has the form of the diffusion equation,

$$[-i\{\omega + \delta\} - D\nabla^2 + \tau_d^{-1}]P_d = \delta(\mathbf{R} - \mathbf{R}'). \quad (5)$$

It contains $\tilde{\omega} = \omega + \delta$ with $\delta = p_F^2 [\gamma(B_{\parallel 1}) - \gamma(B_{\parallel 2})] / 2\hbar$ and the rate

$$\tau_d^{-1} = \frac{\tau p_F^4}{8\hbar^2} [\gamma(B_{\parallel 1}) - \gamma(B_{\parallel 2})]^2 + \frac{2\zeta^2}{\tau} p_F^2 [B_{\parallel 1} - B_{\parallel 2}]^2 \quad (6)$$

The first term in Eq. (6) comes from the deformation of a Fermi circle by B_{\parallel} , the second takes into account the field effect upon the scattering of plane waves. Equation (5) also contains the difference between the electron kinetic energies in two measurements of conductance, $\omega = E_F(B_{\parallel 1}) - E_F(B_{\parallel 2})$, each of them shifted, $E_F(B_{\parallel}) = E_F^0 - \frac{1}{2} p_F^2 \gamma(B_{\parallel})$ with respect to the Fermi energy E_F^0 in the electron gas with the same sheet density at $B_{\parallel} = 0$. The latter fact is important, since, for lateral dots where electron density is fixed, one should substitute $\tilde{\omega} = \omega + \delta = 0$, so that only the B_{\parallel} -dependent anisotropy of the electron wavelength along the Fermi line affects the interference pattern of current carriers.

The Cooperon equation derived after the calculation of the integral in $\Pi(\omega, \mathbf{q})$ can be represented in the form

$$[-i\tilde{\omega} + D(-i\nabla - \mathbf{q})^2 + \tau_C^{-1} + \tau_d^{-1}]P_C = \delta(\mathbf{R} - \mathbf{R}'). \quad (7)$$

It contains an additional decay rate, $\tau_C^{-1}(B_{\parallel 1}, B_{\parallel 2})$,

$$\tau_C^{-1} = \frac{\tau p_F^6}{8\hbar^2} \left[\frac{\beta(B_{\parallel 1}) + \beta(B_{\parallel 2})}{2} \right]^2 + \frac{\zeta^2 p_F^2}{2\tau} [B_{\parallel 1} + B_{\parallel 2}]^2$$

which accounts for dephasing between electrons encircling the same chaotic trajectory in reverse directions, the result of lifting the time-reversal symmetry by an in-plane magnetic field. The corresponding dephasing rate $\tau_{B_{\parallel}}^{-1} = \tau_C^{-1}(B_{\parallel}, B_{\parallel})$,

$$\tau_{B\parallel}^{-1} = \frac{\tau p_F^6}{8\hbar^2} \beta^2(B_{\parallel}) + \frac{2\xi^2 p_F^2 B_{\parallel}^2}{\tau}, \quad (8)$$

can be used when describing the WL correction to the conductivity of 2D electron gases in semiconductor heterostructures and field transistors. The second term in this rate would be dominant in low-mobility structures with strongly asymmetric potential disorder, such as the interface roughness or impurities positioned inside the electron accumulation layer. The first term in Eq. (8) would be the main one in high-mobility structures with carrier scattering at remote charges behind the spacer.

To mention, a shift in the Cooperon gauge in Eq. (7),

$$\mathbf{q} = 3/2\hbar p_F^2 m \beta(B_{\parallel}) [\mathbf{B}_{\parallel} \times \mathbf{l}_z] / B_{\parallel},$$

is the result of the following artifact: cubic term in the effective electron dispersion not only lifts the inversion symmetry of the line $E(B_{\parallel}, \mathbf{p}) = E_F(B_{\parallel})$, but also shifts its geometrical center with respect to the true bottom of the 2D conduction band. Since in conductance calculations only electrons with $E = E_F$ matter, such a shift would be eliminated by choosing a slightly modified initial gauge, which can now be corrected by applying a gauge transformation $P_C = e^{i\mathbf{q} \cdot \mathbf{R}} \bar{P}_C$ directly to the Cooperon. One may say that the phase-coherent transport is only affected by the B_{\parallel} -induced ($\mathbf{p} \rightarrow -\mathbf{p}$)-asymmetric distortion of the Fermi circle into an oval, but not by a shift of such an oval in the momentum space.

Finally, we can apply the rate of time-reversal symmetry breaking due to the in-plane field in Eq. (8) to analyze the WL correction to the quantum dot conductance in Eq. (1), and also the $o \rightarrow u$ crossover in conductance fluctuations under conditions that the magnetic-field direction is finelytuned to have only the in-plane component¹² and the UCF are studied by slightly varying the shape or area of a dot using the multiple gates technique⁸. In a ballistic billiard, or in a heterostructure with z -independent scattering potential, it would be dominated by B_{\parallel}^6 dependence (also found in Ref. 15) that we attribute to the effect of the cubic term generated by B_{\parallel} in the 2D electron dispersion, thus giving rise to a relatively sharp crossover between “flat” regions related to orthogonal and unitary symmetry regimes. For a large-area ($8 \mu\text{m}^2$) quantum dot with electron density $2 \times 10^{11} \text{ cm}^{-2}$ studied by Folk and co-workers,^{5,12} we estimated the crossover field as $B_{\parallel} = 0.6 \div 0.8 \text{ T}$. When studying the crossover, one has to take into account that the in-plane field also causes fluctuations in conductance, without breaking time-reversal symmetry, as described by Eqs. (2,6). For the same parameters of a structure, we estimated the field where such a random dependence would appear as $B_{\parallel} \sim 0.3 \text{ T}$, and the result in Eq. (6) suggests that, for a perfectly in-plane field orientation, variation of the UCF fingerprint is faster at higher fields.

We thank B. Altshuler, C. Marcus and J. Meyer for discussions and for information concerning unpublished works.^{12,15} This research was funded by EPSRC, NATO CLG and EC INTAS.

¹R.A. Webb *et al.*, Phys. Rev. Lett. **54**, 2696 (1985).

²J.C. Licini *et al.*, Phys. Rev. Lett. **55**, 2987 (1985).

³B.L. Altshuler and D.E. Khmel'nitskii, Pis'ma Zh. Éksp. Teor. Fiz. **42**, 291 (1985) [JETP Lett. **42**, 359 (1985)]; P.A. Lee and A.D. Stone, Phys. Rev. Lett. **55**, 1622 (1985); P.A. Lee, A.D. Stone, and H. Fukuyama, Phys. Rev. B **35**, 1039 (1987).

⁴C.W.J. Beenakker, Rev. Mod. Phys. **69**, 731 (1997); Y. Alhassid, *ibid.* **72**, 895 (2000).

⁵J.A. Folk *et al.*, Phys. Rev. Lett. **86**, 2102 (2001).

⁶A.G. Huibers *et al.*, Phys. Rev. Lett. **81**, 200 (1998); A.G. Huibers *et al.*, *ibid.* **83**, 5090 (1999).

⁷U. Sivan *et al.*, Europhys. Lett. **25**, 605 (1994); T. Schmidt *et al.*, Phys. Rev. Lett. **86**, 276 (2001).

⁸I.H. Chan *et al.*, Phys. Rev. Lett. **74**, 3876 (1995).

⁹C.M. Marcus *et al.*, Phys. Rev. B **48**, 2460 (1993).

¹⁰B.I. Halperin *et al.*, Phys. Rev. Lett. **86**, 2106 (2001).

¹¹I. Aleiner and V. Fal'ko, Phys. Rev. Lett. **87**, 256801 (2001).

¹²C. Marcus and J. Folk (private communication).

¹³L. Smrcka *et al.*, Phys. Rev. B **51**, 18 011 (1995); J.M. Heisz and E. Zaremba, *ibid.* **53**, 13594 (1996).

¹⁴I. Kukushkin *et al.*, Pis'ma Zh. Éksp. Teor. Fiz. **53**, 321 (1991) [JETP Lett. **53**, 335 (1991)]; V. Kirpichev *et al.*, Pis'ma Zh. Éksp. Teor. Fiz. **51**, 383 (1990) [JETP Lett. **51**, 436 (1990)].

¹⁵J. Meyer, A. Altland, and B. Altshuler, cond-mat/0105623 (un-

published).

¹⁶Z. Pluhar *et al.*, Phys. Rev. Lett. **73**, 2115 (1994).

¹⁷K.B. Efetov, Phys. Rev. Lett. **74**, 2299 (1995).

¹⁸Using perturbation theory expansion for the plane wave energy, up to the third order in p_{\perp} (assuming that $p_F \langle n|z|0 \rangle < p_F \lambda_z < \hbar$), we arrived at $\delta E = \delta_2 + \delta_3$,

$$\delta_2 \approx -\frac{p_{\perp}^2 B_{\parallel}^2}{m^2} \sum_{n \geq 1} \frac{\langle n|z|0 \rangle^2}{\varepsilon_n - \varepsilon_0} \sim -\frac{p_{\perp}^2}{m} \left(\frac{\lambda_z}{\lambda_B} \right)^4,$$

$$\delta_3 \approx \frac{p_{\perp}^3 B_{\parallel}^3}{m^3} \sum_{k, n \geq 1} \frac{\langle 0|z|k \rangle \langle k|z|n \rangle \langle n|z|0 \rangle}{[\varepsilon_k - \varepsilon_0][\varepsilon_n - \varepsilon_0]} \sim \frac{p_{\perp}^3 \lambda_z}{m \hbar} \left(\frac{\lambda_z}{\lambda_B} \right)^6,$$

where $\lambda_B = \sqrt{\hbar c / e B_{\parallel}}$ is the magnetic length.

¹⁹S.H. Vosko, L. Wilk, and M. Nusair, Can. J. Phys. **58**, 1200 (1980).

²⁰V. I. Fal'ko, J. Phys.: Condens. Matter **2**, 3797 (1990); V. I. Fal'ko, Phys. Rev. B **50**, 17 406 (1994).

²¹H. Mathur and H.U. Baranger, cond-mat/0008375 (unpublished).

²²K.B. Efetov, *Supersymmetry in Disorder and Chaos* (Cambridge University Press, Cambridge, 1997).

²³R.A. Jalabert, H.U. Baranger, and A.D. Stone, Phys. Rev. Lett. **65**, 2442 (1990).

²⁴R.A. Serota *et al.*, Phys. Rev. B **36**, 5031 (1987).